Adaptive beamforming for large arrays in satellite communications systems with dispersed coverage

J. Montesinos[1,2] O. Besson[1] C. Larue de Tournemine[2]

[1]*University of Toulouse, ISAE/TéSA, 10 Avenue Edouard Belin, 31055 Toulouse, France*
[2]*Thales Alenia Space, 26 Avenue J.-F. Champollion, France*
E-mail: olivier.besson@isae.fr

Abstract: Conventional multibeam satellite communications systems ensure coverage of wide areas through multiple fixed beams where all users inside a beam share the same bandwidth. The authors consider a new and more flexible system where each user is assigned his own beam, and the users can be very geographically dispersed. This is achieved through the use of a large direct radiating array coupled with adaptive beamforming so as to reject interferences and to provide a maximal gain to the user of interest. New fast-converging adaptive beamforming algorithms are presented, which allow one to obtain good signal to interference and noise ratio with a number of snapshots much lower than the number of antennas in the array. These beamformers are evaluated on reference scenarios.

1 Introduction

Satellite telecommunications systems specified today require high-gain satellite antennas to supply sufficient link budgets towards small user terminals. In this context, satellite on-board multiple beam antennas (MBA) have been successfully employed either for personal communications, military communications or Internet applications [1]. They allow one to insure high gain by means of multiple adjacent patterns covering an extended zone. They also allow one to introduce some frequency reuse on non-adjacent beams, thereby increasing the available capacity for a given bandwidth.

Standard MBA provide a fixed coverage with adjacent beams crossing typically 3–4 dB below maximum gain level. They are associated to a fixed bandwidth to beam allocation, with typical 1:3 or 1:4 frequency reuse scheme, that is to say, the frequency is reused on one beam over three or four. On classical payloads, beamforming is performed in radio frequency domain, prior to channelisation function (usually on intermediate frequency or in digitised baseband). By introducing digital beamforming networks associated to transparent or regenerative processor, the interest of such a multibeam antenna can be considerably improved. As a matter of fact, digital beamforming allows one to introduce fully flexible beamforming. Moreover, by crossing on board beamforming functions with channelisation, it becomes possible to introduce some flexibility in terms of bandwidth to beam allocation. Finally, the coverage reconfigurability offered by digital beamforming associated to flexible channelisation makes it possible to set capacity where required when required, thus adapting the provided resources to effective traffic requirements [2, 3].

When considering a moderate bandwidth, it is possible to generalise this flexible approach, and go towards a 'one beam per user' concept within a reasonable on board processing complexity. In such a system, a suited capacity (i.e. bandwidth) can be attributed to each user, or to a small group of users. A specific beam, pointed towards the user of interest (UOI), provides the maximum gain made available by the antenna aperture, thus improves the link budget by up to 3 or 4 dB with regard to traditional multibeam coverage where edge of coverage gain must be considered. Furthermore, if considering several users associated to the same radio resource, it is possible to

adaptively form the beams associated to each of these users, in order to reject specifically co-users interferences. The rejection of interfering signals results in a significantly improved signal-to-interference and noise ratio (SINR) for each user, as compared to standard solution where antenna pattern sidelobes are minimised over an extended zone.

Thanks to combined gain improvement, and isolation enhancement, the obtained SINR on each link can then be dramatically increased with regard to the performance obtained with a standard coverage provided by an equivalent antenna aperture. The improved SINR can lead to increase effective payload throughput by using more efficient modulation and coding scheme on user to satellite link. Alternatively, keeping given SINR specification, the system capacity can be improved by increasing cumulated processed bandwidth. As a matter of fact, the adapted isolation between users makes it possible to reuse frequency on closer users than what was made possible with standard systems. However, to provide significant improvement by properly pointing and shaping antenna patterns, it is necessary to introduce some adaptive antenna beamforming.

It has been shown in previous works [4, 5] that digital beamforming antenna can provide flexible beams to individual users on demand. The combination of both adaptive processing and a suited resource allocation scheme ensure the best use of available capacity. We can then refer to space division multiple access (SDMA). Frequency channels are reused as much as made possible by antenna spatial filtering capacity. The allocation process highly impacts final capacity, but the optimisation of such algorithm is outside the scope of the present paper. However in [4], the restricted area covered by the antenna (about 1000 km wide) leads one to use a focal array antenna including few radiating elements, thus few array controls. The associated adaptive array processing then stays within a reasonable complexity, and no specific effort was set on considering adaptive algorithm optimisation in terms of computational cost.

In this paper, we study the reception antenna of a geostationary satellite communication system, operating in Ka-band, which must provide high-gain beams towards users located anywhere on the visible earth surface. We present in the first part of the paper the constraints that are associated with such a coverage, and show that the antenna design leads to a radiating panel including a large number of controls. The classical adaptive beamforming methods such as those considered in [4–6] are then not suited any more, as leading to excessive complexity. The second part of the paper is then devoted to the description of specific adaptive beamforming algorithms that allow one to avoid array elements covariance matrix inversion and work in a low-dimensional subspace. This matrix can thus be estimated with a much reduced number of samples, without affecting adaptive processing convergence leading to a dramatic reduction of the algorithm associated complexity and number of acquisitions. Finally, the last part of the paper presents simulation results illustrating the performances expected in a reference scenario.

2 Antenna design and constraints related to adaptive beamforming

2.1 Coverage constraints and associated antenna design

We here consider a 'one beam per user' coverage. Beams are digitally formed by applying proper weighting, after prior channelisation of the signal sampled after each radiating element. The same radio resource can be used in several beams as long as spatial filtering allows separating associated signals. Beams are pointed individually towards each user, thus the gain provided in the direction of the user is maximised with regard to antenna size. Users can be placed anywhere on visible side of the Earth as seen from a geostationary satellite. Locally contiguous coverage can be needed implying isolation capacity requirement. Isolated users can also be covered. Fig. 1 gives an example of the coverage that can be needed and illustrates time-frequency resources reuse for close users. The square represents the UOI. The UOI is assumed to share the same resource as the co-users represented here by full circles, whereas the diamonds are the symbols of users of the system sharing a different resource. Finally, the cross symbolises a jamming station for the UOI.

The system has to work, even if intentional or unintentional interferences or jammers are active in the coverage. If users are sharing a resource (the same frequency channel for instance), they are interfering with each other. Intentional jamming stations may also be present. We consider here that jammers are acting like

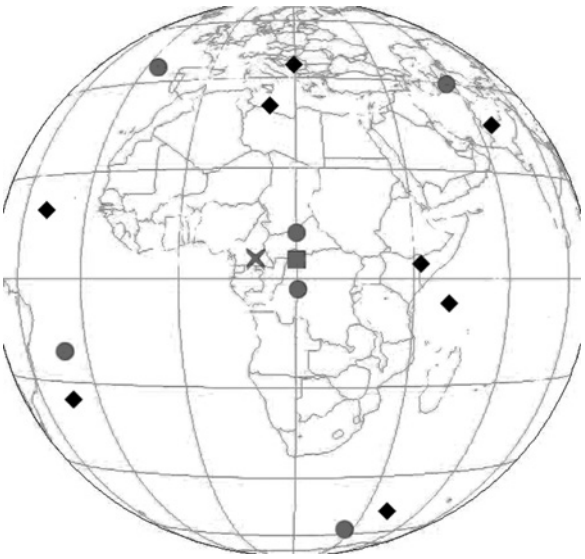

Figure 1 *Example of required coverage*

co-users interferences, except that their power is much higher (typ. 10 dB).

The simplest way to implement an MBA is to provide each beam with a single radiating element, located at the focal plane of an optical device (single or multiple reflectors). However, such an implementation cannot provide a continuous multiple beam coverage with high efficiency. As a matter of fact, the inter-feed spacing is driven by beam spacing requirement. The allowable feed size is then small, leading to non-optimum illumination of the reflector and degraded performances for edge of coverage gain. To obtain sufficient performances, one possible solution is to use three or four 'one feed per beam' antennas, having their beam lattice interleaved. The feed size is then allowed one to increase, without compromising beam spacing. Three or four reflector antennas must be used to provide the complete coverage. In addition to its bulkiness, the main issue of such a solution lies in its lack of flexibility, since no beam reconfigurability is possible.

Another solution to provide multiple beams, using only one reflector, is to use overlapping sub-arrays to increase the effective aperture of each equivalent feed. The focalising device associated with the array can be a single or a double reflector. The array fed reflector (AFR) beams are generated by combining signals coming from clusters of typically 7–19 active feeds per beam depending on gain and inter-beam isolation specifications. As compared to a 'one feed per beam' solution using identical focalising device, the C/I ratio (power received from the nominal beam, divided by that coming from the ones which interfere in the same sub-band) can be increased by 3–5 dB. Each feed contributes to several beams, typically 1 to 7, for central feeds. The total number of feeds of the antenna is mainly related to the global extension of the coverage. Such antennas are privileged for moderately extended coverage (typically Europe or the contiguous USA) or when lower-frequency reuse scheme are required. For instance, Inmarsat 4 satellite uses a seven colours frequency reuse scheme [7]. It is, however, difficult to provide both high gain and rejection capacity on a widely extended coverage as required in our application with such an antenna.

Finally, the best antenna solution to provide multiple high-gain beams spread all over Earth coverage without compromising spatial filtering capacity for close users is a direct radiating antenna (DRA). In such an antenna, each radiating element contributes to every beam. In addition to being well suited to the coverage requirements, such a phased array antenna is also attractive, as it is likely to reduce the dynamics of beamforming network signal, which is critical for DBFN implementation. Furthermore the graceful degradation principle avoids the '2 per 1' redundancy, which is very expensive for antenna receiving devices. For an example of system using a DRA, there is the WINDS satellite which has two 128 elements DRA, aiming at covering the Asia-Pacific region with four reconfigurable beams (two for transmission and two for reception) using analogue BFN [8].

Designing a DRA radiating panel mainly consists in considering the two following constraints [9]:

- Antenna diameter is mainly determined by minimum directivity level, which must be insured for all users of the coverage, in order to comply with link budget requirements.

- Grid lattice is constrained by grating lobe rejection outside a given domain (typically outside the Earth, for a geostationary satellite antenna considered here), to avoid losses and possible interferences related to grating lobes. The maximum size of radiating elements is then related to coverage global extension, defining maximum beam pointing angle.

For our particular case, both high gain and extended coverage are required. DRA sizing for geostationary satellite and extended coverage lead typically to a number of radiating elements going from one to a few hundreds. Some solutions are investigated to reduce the number of controls used in the beamforming process either by thinning the array, or by introducing a first stage of analogue beamforming. The irregular subarray division allows one to break lattice periodicity, thus avoids grating lobes keeping a reduced number of digital controls [10]. However, for our case, the remaining number of control stays too important to use classical beamforming techniques. Indeed, complexity of usual adaptive algorithms issues become a bottleneck for SDMA-like implementation. We here briefly review conventional full-dimension adaptive beamforming techniques, prior to presenting the solutions that could allow for fast convergence at a low computational cost.

2.2 Adaptive beamforming

Adaptive beamforming consists in spatially filtering the received array data with a view to recover a signal of interest (SOI) while eliminating the interferences that could possibly be present. This area has been extensively studied in recent years and numerous solutions have been proposed, see for example [11] for a thorough review. The optimal beamformer amounts to solving the following minimisation problem

$$\min_{\boldsymbol{w}} \boldsymbol{w}^H \boldsymbol{R} \boldsymbol{w}, \quad \text{subject to } \boldsymbol{w}^H \boldsymbol{v} = 1 \tag{1}$$

where $\boldsymbol{v}$ is the spatial signature of the SOI and $\boldsymbol{R}$ is the covariance matrix of the array output. The constraint in (1) guarantees that the SOI will be undistorted after beamforming, and because of the minimisation of the output power, the beamformer will tend to place nulls towards the interferences in order to reduce their contribution. When the array measurements contain the

interferences and noise only, $\boldsymbol{R} = \boldsymbol{R}_{\text{i+n}}$ where $\boldsymbol{R}_{\text{i+n}}$ denotes the interferences plus noise covariance matrix, and the beamformer is usually referred to as the minimum variance distortionless response (MVDR) beamformer. When the SOI is also present in the measurements, $\boldsymbol{R} = \boldsymbol{R}_{\text{i+n}} + P\boldsymbol{v}\boldsymbol{v}^H$ and the terminology minimum power distortionless response (MPDR) beamformer is used [11]. Whatever the value of $\boldsymbol{R}$, the solution to (1) is given by [11]

$$\boldsymbol{w}_{\text{opt}} = \frac{\boldsymbol{R}^{-1}\boldsymbol{v}}{\boldsymbol{v}^H\boldsymbol{R}^{-1}\boldsymbol{v}} \tag{2}$$

When the covariance matrix is known, $\boldsymbol{w}_{\text{opt}}$ is the same whether $\boldsymbol{R} = \boldsymbol{R}_{\text{i+n}}$ or $\boldsymbol{R} = \boldsymbol{R}_{\text{i+n}} P\boldsymbol{v}\boldsymbol{v}^H$ and the optimal beamformer enables one to achieve the optimal SINR

$$\text{SINR}_{\text{opt}} = P\boldsymbol{v}^H\boldsymbol{R}_{\text{i+n}}^{-1}\boldsymbol{v} \tag{3}$$

where P stands for the SOI power. At this point, we would like to emphasise a significant difference between the two beamformers. The MVDR beamformer requires that data, free of the SOI, be available, which may be a major constraint in communications systems. Hence, specific access schemes need to be planned in order to obtain SOI-free measurements and to implement the MVDR beamformer. In contrast, this requirement does not hold for the MPDR beamformer.

In practical situations, $\boldsymbol{R}$ is not known and is estimated from N available snapshots $\boldsymbol{X} = [\boldsymbol{x}(1)\ \boldsymbol{x}(2)\ \cdots\ \boldsymbol{x}(N)]$ as

$$\hat{\boldsymbol{R}} = N^{-1}\boldsymbol{X}\boldsymbol{X}^H = N^{-1}\sum_{t=1}^{N}\boldsymbol{x}(t)\boldsymbol{x}^H(t) \tag{4}$$

with the latter referred to as the sample covariance matrix (SCM). When the number of snapshots N is larger than the number of array elements m, that is $N > m$, the SCM is invertible with probability 1 and one usually substitutes $\boldsymbol{R}$ for the SCM in (2) to yield

$$\boldsymbol{w}_{\text{smi}} = \frac{\hat{\boldsymbol{R}}^{-1}\boldsymbol{v}}{\boldsymbol{v}^H\hat{\boldsymbol{R}}^{-1}\boldsymbol{v}} \tag{5}$$

where the subscript 'smi' stands for sample matrix inversion. The computational complexity associated with (5) depends on the number of snapshots N and the number of elements m since one needs to invert a $m \times m$ matrix. Therefore considerable effort has been devoted to design beamformers that can provide good SINR with a limited number of snapshots and at a low computational cost. A commonly admitted criterion is the so-called convergence measure of effectiveness (MOE), that is the number of snapshots required for a beamformer to achieve–on average–the optimal SINR (3) within 3 dB. The MOE directly impacts the computational load as well as the rate at which the beamformer can be updated, in case of non-stationary environments for instance. The MOE of the MVDR is significantly lower than that of the MPDR when using the SCM. Since the landmark paper by Reed Mallett and Brennan [12], it is known that the MOE of the MVDR is approximately $2m - 3$ snapshots. In contrast, for the same performance, $2m - 3 + (m-1)\text{SINR}_{\text{opt}}$ snapshots are necessary [11, 13, 14], which is prohibitive in most applications. We would also like to stress that, in the case $N < m$ we consider in this paper, the beamformer in (5) is even not implementable as $\hat{\boldsymbol{R}}$ is not invertible, actually its rank is N. The methods we are looking for should, once again, avoid the estimated covariance matrix inversion while keeping a good MOE.

3 Low-complexity adaptive beamforming

In order to improve the beamformer MOE, several strategies have been proposed in the literature. Our aim here is not to provide an exhaustive review of them, rather to sample the most widely used and most effective techniques. A premier choice is diagonal loading [15] which consists in adding a scaled identity matrix to $\hat{\boldsymbol{R}}$ before inversion, yielding

$$\boldsymbol{w}_{\text{dl}} = \frac{(\hat{\boldsymbol{R}} + \sigma_{\text{dl}}^2\boldsymbol{I})^{-1}\boldsymbol{v}}{\boldsymbol{v}^H(\hat{\boldsymbol{R}} + \sigma_{\text{dl}}^2\boldsymbol{I})^{-1}\boldsymbol{v}} \tag{6}$$

The above beamformer can be implemented even for $N \leq m$, its MOE is commensurate with twice the number of interferences J, and it is thus very effective. The drawback of such a method lies in the fact that it is not always simple to fix the diagonal loading level σ_{dl}^2 although some ways to fix it, either adaptively or automatically have been proposed, see for example [16–18]. Additionally, the inversion of a $m \times m$ covariance matrix is still required, which is computationally intensive for large m.

A second and important class of fast-converging beamformers consists of the so-called reduced-rank (RR) beamformers [19, 20] whose principle is to operate in a subspace of the measurements, hence reducing the size of the observations, and subsequently the sample support required. They exploit the fact that the interferences occupy a subspace that can be estimated by eigenvalue decomposition (EVD) of the covariance matrix. In this category, the more widely known methods are the principal components (PC) method [21, 22] and the cross-spectral metric method (CSM) [23]. Although their MOE is of the order of $2J$, and they do not require directly a matrix inversion, these methods are still computationally intensive as they require the EVD of $\hat{\boldsymbol{R}}$. Given the scenario we consider in this paper–large number of elements m and small number of snapshots $N \ll m$–we are looking for methods whose MOE is of the order $2J$ without requiring the inversion of a large matrix or its EVD. Hence, the methods listed above are not entirely satisfactory and we now focus on three recently proposed approaches which can meet our requirements.

3.1 Conjugate gradient (CG) beamformer

The CG is a well-known technique to solve linear systems of equations such as $\boldsymbol{R}\boldsymbol{w} = \boldsymbol{v}$ [24]. It enables to obtain the solution in m steps without any matrix inversion and is thus computationally attractive. For the sake of convenience, a possible implementation of the CG beamformer is displayed in Fig. 2. As for all algorithms, the input matrix $\boldsymbol{R}$ should be considered as a "generic" input matrix, keeping in mind that it can correspond to the covariance matrix of interferences plus noise (MVDR scenario) or the covariance matrix of the SOI, the interferences and the noise (MPDR scenario). Moreover, in practice all algorithms considered will use $\hat{\boldsymbol{R}}$ in place of $\boldsymbol{R}$ as input. In fact, the CG algorithm was not really used to obtain the MVDR solution until its connection with the multi-stage Wiener filter (MWF) [25] was discovered [26]. The MWF is an RR filter in which the RR subspace is determined by maximising cross-correlations between the desired signal and the observed data. Therefore in contrast to PC or CSM, it does not require EVD. Yet, its performance was shown to be generally better than that of PC and CSM with a possibly smaller MOE. The MWF was found to operate in the Krylov subspace $\mathcal{K}(\boldsymbol{v}, \boldsymbol{R}, n) = \mathcal{R}\{\boldsymbol{v}, \boldsymbol{R}\boldsymbol{v}, \ldots, \boldsymbol{R}^{n-1}\boldsymbol{v}\}$ where $\mathcal{R}\{\cdot\}$ stands for the range space, hence its connection with the CG since the latter, at iteration n, is known to operate in this subspace.

In Fig. 2, the iterations should be run till $r = m$ to solve $\boldsymbol{R}\boldsymbol{w} = \boldsymbol{v}$. However, as explained now, it may be recommended to stop the iterations earlier. If the covariance matrix contains J interferences with high interference to noise ratio (INR), its EVD can be written as $\boldsymbol{R} = \boldsymbol{U}_i\boldsymbol{\Lambda}_i\boldsymbol{U}_i^H + \sigma^2\boldsymbol{U}_n\boldsymbol{U}_n^H$ with $\boldsymbol{\Lambda}_i = \mathrm{diag}(\lambda_1, \ldots, \lambda_J)$ and $\lambda_k \gg \sigma^2$. It follows that $\boldsymbol{R}^n \simeq \boldsymbol{U}_i\boldsymbol{\Lambda}_i^n\boldsymbol{U}_i^H$ and hence, at iteration $n = J + 1$, the Krylov subspace will capture the interference subspace: the filter will then be most effective in rejecting the interferences. In other words, Fig. 2 should not be necessarily run until $n = \min(m, N)$ but should be stopped at $n = J + 1$ where the SINR will be maximum. In fact, when using $\hat{\boldsymbol{R}}$ instead of $\boldsymbol{R}$, it has been observed that the SINR generally decreases when n is increased above $J + 1$ and tends to that of $\boldsymbol{w}_{\mathrm{smi}}$ in (5), provided that $\hat{\boldsymbol{R}}$ is invertible. The problem is that in practical situations one does not know exactly the number of interfering signals. On one hand, one should not stop before $n = J + 1$ as all interferences will not be suppressed. On the other hand, a too large r will result in poorer SINR, especially if a rank deficient $\hat{\boldsymbol{R}}$ is used in Fig. 2. In order to remedy this problem, we propose to include diagonal loading directly in the CG beamformer, and refer to as the CG–DL beamformer. This simply amounts to replacing $\boldsymbol{R}$–actually $\hat{\boldsymbol{R}}$–by $\hat{\boldsymbol{R}} + \sigma_{\mathrm{dl}}^2\boldsymbol{I}$ in line 1 of Fig. 2. Although the modification is minor, it yields considerable improvement. Indeed, one does not need to know J, only an upper bound for this value. In contrast to the original CG, choosing $r > J + 1$ does not result in a decrease of the SINR in a MPDR-type scenario. In fact, we observed, by varying r, that the SINR is generally optimum at $r = J + 1$ but then tends to be rather constant. Moreover, when one uses the SCM and the latter is rank deficient (because of $N < m$), one does not encounter any numerical problem as the inverse of $\hat{\boldsymbol{R}} + \sigma_{\mathrm{dl}}^2\boldsymbol{I}$ exists whatever N. This fact will be illustrated in the next section.

3.2 Auxiliary vector (AV) beamformer

The AV beamformer was introduced in [27] as a simple solution to compute the MVDR solution without resorting to any matrix inversion. The implementation of the AV beamformer is described by Fig. 3 where $\boldsymbol{P}_{\boldsymbol{v}}^{\perp}$ in line 3 of Fig. 3 stands for the orthogonal projector onto the subspace orthogonal to $\boldsymbol{v}$. The basic idea behind this algorithm is to build, at each iteration step n, an AV $\boldsymbol{g}_n$ which is orthogonal to $\boldsymbol{v}$. This AV is able to capture the

Algorithm 1
Input: $\boldsymbol{R}$, $\boldsymbol{v}$

1: $w_0 = \boldsymbol{0}$, $\beta_1 = 0$, $\boldsymbol{u}_1 = \boldsymbol{e}_0 = \boldsymbol{v}$
2: **for** $n = 1, \cdots, r$ **do**
3: **if** $n > 1$ **then**
4: $\beta_n = \|\boldsymbol{e}_{n-1}\|^2 / \|\boldsymbol{e}_{n-2}\|^2$
5: $\boldsymbol{u}_n = \boldsymbol{e}_{n-1} + \beta_n \boldsymbol{u}_{n-1}$
6: **end if**
7: $\boldsymbol{z}_n = \boldsymbol{R}\boldsymbol{u}_n$
8: $c_n = \|\boldsymbol{e}_{n-1}\|^2 / \boldsymbol{u}_n^H \boldsymbol{z}_n$
9: $\boldsymbol{e}_n = \boldsymbol{e}_{n-1} - c_n \boldsymbol{z}_n$
10: $\boldsymbol{w}_n = \boldsymbol{w}_{n-1} + c_n \boldsymbol{u}_n$
11: **end for**

Output: sequence of beamformers $\boldsymbol{w}_n$

Figure 2 *CG beamformer*

Algorithm 2
Input: $\boldsymbol{R}$, $\boldsymbol{v}$

1: $\boldsymbol{w}_0 = \left(\boldsymbol{v}^H\boldsymbol{v}\right)^{-1}\boldsymbol{v}$
2: **for** $n = 1, \cdots, r$ **do**
3: $\boldsymbol{g}_n = \boldsymbol{P}_{\boldsymbol{v}}^{\perp}\boldsymbol{R}\boldsymbol{w}_{n-1}$
4: **if** $\boldsymbol{g}_n = \boldsymbol{0}$ **then**
5: exit
6: **else**
7: $\mu_n = \left(\boldsymbol{g}_n^H\boldsymbol{R}\boldsymbol{w}_{n-1}\right) / \left(\boldsymbol{g}_n^H\boldsymbol{R}\boldsymbol{g}_n\right)$
8: $\boldsymbol{w}_n = \boldsymbol{w}_{n-1} - \mu_n\boldsymbol{g}_n$
9: **end if**
10: **end for**

Output: sequence of beamformers $\boldsymbol{w}_n$

Figure 3 *AV beamformer*

most (in sense of maximum magnitude cross-correlation) of the interferences present at the previous iteration filter output. In [27], it was shown that, with $\boldsymbol{R}$ a positive definite covariance matrix, the AV weight vector converges to $\boldsymbol{w}_{\text{opt}}$ in (2) as r goes to infinity. In fact, the AV weight vector comes very close to its limit for a relatively small number of iterations, and a procedure to select the value of r in Fig. 3 was presented in [28]. In finite samples, that is when using $\hat{\boldsymbol{R}}$ instead of $\boldsymbol{R}$, the AV beamformer was shown to have performances commensurate with those of the CG beamformer [29] and is thus a method to consider for our problem. However, the proof of convergence in [27] is based on the fact that the input matrix $\boldsymbol{R}$ is positive definite. When $\hat{\boldsymbol{R}}$ is used this implies that $N > m$. In the case of most interest to us, $N \leq m$ and hence $\hat{\boldsymbol{R}}$ has rank N. In [30], we proved that if the input matrix $\boldsymbol{R}$ of Fig. 3 is rank deficient, with EVD $\boldsymbol{R} = \boldsymbol{U}\boldsymbol{\Lambda}\boldsymbol{U}^H$ where $\boldsymbol{U} = [\boldsymbol{u}_1\ \boldsymbol{u}_2\ \cdots\ \boldsymbol{u}_p] \in \mathbb{C}^{m\times p}$ is a unitary matrix, then the limit of the weight vector $\boldsymbol{w}_n$ of Fig. 3 is

$$\lim_{n\to\infty} \boldsymbol{w}_n = \frac{\boldsymbol{U}_\perp \boldsymbol{U}_\perp^H \boldsymbol{v}}{\boldsymbol{v}^H \boldsymbol{U}_\perp \boldsymbol{U}_\perp^H \boldsymbol{v}} \triangleq \boldsymbol{w}_{\text{AV}-\infty} \tag{7}$$

where $\boldsymbol{U}_\perp$ is an orthonormal basis for $\mathcal{R}\{\boldsymbol{U}\}^\perp$.

First observe that this limit belongs to a low-rank subspace, and hence the AV beamformer asymptotically (in n) belongs to the class of RR beamformers. Hence it should inherit their properties in terms of low MOE. Moreover, it enables one to achieve effective interference cancellation. As explained in [30], in a MVDR scenario, the columns of $\boldsymbol{U}_\perp$ will mostly lie in the null space of the interferences, that is, $\boldsymbol{U}_\perp^H \boldsymbol{A}_{\text{i}} \simeq 0$, where the columns of $\boldsymbol{A}_{\text{i}} \in \mathbb{C}^{m\times J}$ are the interferences steering vectors. In an MPDR-type scenario, the SOI is also present. In the absence of noise, the matrix $\boldsymbol{X}$ has rank $J+1$ for $N \geq J+1$, and its range space is $\mathcal{R}\{\boldsymbol{X}\} = \mathcal{R}\{[\boldsymbol{v}\quad \boldsymbol{A}_{\text{i}}]\}$. It follows that $\boldsymbol{U}_\perp$ will be orthogonal to both $\boldsymbol{v}$ and $\boldsymbol{A}_{\text{i}}$, which is desirable for $\boldsymbol{A}_{\text{i}}$ but is to be avoided for $\boldsymbol{v}$. In the presence of noise, the rank of $\hat{\boldsymbol{R}}$ is again N and most of the energy of $\boldsymbol{v}$ and $\boldsymbol{A}_{\text{i}}$ will be confined in $\boldsymbol{U}$. It follows that, in a MPDR scenario, the asymptotic vector $\boldsymbol{w}_{\text{AV}} - \infty$ may not be advocated. However, in order to balance the previous comment, one should mention that usually the iterations are not run until convergence, mainly because convergence may be very slow and thus the corresponding computational cost becomes prohibitive. In fact, the transient behaviour of Fig. 3 is more interesting. Indeed, in order to keep the computational cost low, r is chosen relatively small. Moreover, it can be observed, see the next section, that the beamformer obtained after a few iterations has a better performance than the asymptotic beamformer, especially in a MPDR scenario.

3.3 Random beamspace processing

Beamspace processing is a usual way to operate in a low-dimensional subspace [11]. It consists in applying first a beamspace transformation on the data, that is, $\boldsymbol{x} \to \tilde{\boldsymbol{x}} = \boldsymbol{\Phi}^H \boldsymbol{x}$ where $\boldsymbol{\Phi}$ is a $m \times r$ matrix and then in computing the adaptive weight in the transformed space, that is, in solving

$$\min_{\tilde{\boldsymbol{w}}} \tilde{\boldsymbol{w}}^H \tilde{\boldsymbol{R}} \tilde{\boldsymbol{w}}, \quad \text{subject to } \tilde{\boldsymbol{w}}^H \tilde{\boldsymbol{v}} = 1 \tag{8}$$

where $\tilde{\boldsymbol{v}} = \boldsymbol{\Phi}^H \boldsymbol{v}$ and $\tilde{\boldsymbol{R}} = \boldsymbol{\Phi}^H \boldsymbol{R} \boldsymbol{\Phi}$. The solution to the above problem is obviously

$$\tilde{\boldsymbol{w}} = \frac{\tilde{\boldsymbol{R}}^{-1}\tilde{\boldsymbol{v}}}{\tilde{\boldsymbol{v}}^H \tilde{\boldsymbol{R}}^{-1} \tilde{\boldsymbol{v}}} \tag{9}$$

and the 'equivalent' beamformer is $\boldsymbol{\Phi}\tilde{\boldsymbol{w}}$. Note that the only matrix to be inverted is $\tilde{\boldsymbol{R}}$ whose dimension is $r \times r$, and r is typically small. Usually, the columns of the transformation matrix $\boldsymbol{\Phi}$ are steering vectors, and the corresponding beams should let the SOI pass undistorted and capture the interferences. When these conditions are met, such a technique is very efficient from a computational point of view and effective in terms of MOE. However, the directions of the interfering signals are seldom known and fixing $\boldsymbol{\Phi}$ a priori is a delicate issue. Of course, the beamspace transformation can be chosen adaptively, for example, from the largest eigenvectors of the covariance matrix, but, as said previously, we wish to avoid such EVD. An interesting alternative, suggested in [31], is to select random unitary matrices $\boldsymbol{\Phi}$ and to average the corresponding beamformers, so as to benefit from a diversity effect.

In [31], the technique was used for direction finding problems and the idea is to average, over a certain number of random $\boldsymbol{\Phi}$, the output power after beamspace processing. This method can work with singular covariance matrices – which is our case herein – and avoids diagonal loading and the problem of choosing the loading level. It was shown to perform well with a number of snapshots smaller than the number of array elements. In this paper, we adapt this idea to the problem of designing a beamformer. Since the transformation is constrained to let the SOI pass through undistorted, the matrix $\boldsymbol{\Phi}$ can be chosen as

$$\boldsymbol{\Phi} = \left[\tfrac{\boldsymbol{v}}{\|\boldsymbol{v}\|}\quad \boldsymbol{\phi}_2\quad \cdots\quad \boldsymbol{\phi}_r\right] \tag{10}$$

where $\boldsymbol{\phi}_2, \ldots, \boldsymbol{\phi}_r$ are mutually orthonormal beams and are orthogonal to $\boldsymbol{v}$. Let $\boldsymbol{Q}$ be a unitary matrix that rotates $\boldsymbol{v}$ into the first component, that is, $\boldsymbol{Q}^H \boldsymbol{v} = \|\boldsymbol{v}\|[1\quad 0\quad \cdots\quad 0]^{\text{T}} = \|\boldsymbol{v}\|\boldsymbol{e}_1$. Then, $\boldsymbol{\Phi}$ can be written as

$$\begin{aligned}\boldsymbol{\Phi} &= [\boldsymbol{Q}\boldsymbol{e}_1\quad \boldsymbol{\phi}_2\quad \cdots\quad \boldsymbol{\phi}_r] \\ &= \boldsymbol{Q}[\boldsymbol{e}_1\quad \boldsymbol{Q}^H\boldsymbol{\phi}_2\quad \cdots\quad \boldsymbol{Q}^H\boldsymbol{\phi}_r] \\ &= \boldsymbol{Q}\begin{bmatrix} 1 & \boldsymbol{0}_{r-1}^T \\ \boldsymbol{0}_{m-1} & \boldsymbol{\Psi}\end{bmatrix}\end{aligned} \tag{11}$$

where $\boldsymbol{\Psi}$ is an $m-1 \times r-1$ unitary matrix, which is unconstrained, and chosen isotropically random. For

Algorithm 3
Input: $\boldsymbol{R}$, $\boldsymbol{v}$, r

1: $\boldsymbol{w}_{\text{ub}} = \boldsymbol{0}$
2: **for** $\ell = 1, \cdots, L$ **do**
3: generate $\boldsymbol{\Psi}$ according to (12)
4: compute $\boldsymbol{\Phi}$ according to (11)
5: compute $\tilde{\boldsymbol{w}}$ of (9)
6: $\boldsymbol{w}_{\text{ub}} = \frac{1}{\ell}\boldsymbol{\Phi}\tilde{\boldsymbol{w}} + \frac{\ell-1}{\ell}\boldsymbol{w}_{\text{ub}}$
7: **end for**

Output: $\boldsymbol{w}_{\text{ub}}$

Figure 4 *UB beamformer*

instance, $\boldsymbol{\Psi}$ can be generated from a $m-1 \times r-1$ matrix $\boldsymbol{W}$ with independent and identically distributed Gaussian entries as

$$\boldsymbol{\Psi} = \boldsymbol{W}(\boldsymbol{W}^H\boldsymbol{W})^{-1/2} \tag{12}$$

Once $\boldsymbol{\Psi}$ is drawn, the beamforming transformation $\boldsymbol{\Phi}$ is applied to the data, and the corresponding beamspace weight vector $\tilde{\boldsymbol{w}}$ is computed, as well as the equivalent weight vector $\boldsymbol{\Phi}\tilde{\boldsymbol{w}}$. The latter is averaged over multiple realisations with different matrices $\boldsymbol{\Psi}$ to yield the final beamformer, which we refer to as the unitary beamspace (UB) beamformer. The steps involved can thus be summarised by Fig. 4.

The three presented algorithms are potential solutions for an adaptive algorithm implementation on an antenna with a high number of elements. We are now going to assess their performances in a particular scenario.

4 Numerical results

4.1 Antenna design and simulation scenarios

In this section, we illustrate the performances of the beamformers described above: we compare the CG beamformer, with possibly diagonal loading, the AV beamformer, the UB beamformer and the asymptotic AV beamformer, based on their output SINR, which is defined as

$$\text{SINR} = \frac{P|\boldsymbol{w}^H\boldsymbol{v}|^2}{\boldsymbol{w}^H\boldsymbol{R}_{\text{i+n}}\boldsymbol{w}} \tag{13}$$

The latter is averaged over 1000 independent Monte-Carlo trials where, for each trial, a different data matrix $\boldsymbol{X}$ is drawn randomly and a weight vector $\boldsymbol{w}$ is calculated as well as the corresponding SINR in (13). In addition, we also display the worst-case (over 1000 independent Monte-Carlo trials) SINR. Each SINR is plotted in decibels. We will particularly investigate:

1. the influence of r, that is the number of iterations at which Fig. 2 –the CG beamformer– and Fig. 3 –the AV beamformer– are stopped. It should be recalled that r also corresponds to the dimension of the subspace where the CG and UB weight vectors lie.

2. the influence of the number of snapshots N.

We distinguish two scenarios, a MVDR-type scenario where the array data contain only the interferences and the noise and a MPDR-type scenario where, in addition to interferences and noise, the SOI is also present. Note that a MVDR scenario can be a serious constraint for some communications systems, since the communication needs to be interrupted to obtain SOI-free data matrices. The reasons for this distinction are that the output SINRs will be significantly different but corresponds to different operating modes. Analysis show that the relative performance between the beamformers might be different in both cases.

To this aim, we consider a 1.2 m wide circular DRA with $m = 401$ non-isotropic elements, each of them of size $5.7\lambda \times 4.93\lambda$, that are distributed on a triangular grid at 30 GHz (reception mode), see Fig. 5. The maximum possible gain provided by the array is 50.8 dB and the half-power beam-width is 0.43°. We deliberately chose an array of several hundreds of radiating elements to illustrate a case where the computational is highly critical. The array is also chosen to provide a high gain all over the visible earth.

We consider a scenario where the UOI is located in the (u, v)–space at $u_0 = v_0 = 0$, where $u = \sin(\theta)\cos(\phi)$, $v = \sin(\theta)\sin(\phi)$ and θ, ϕ stand, respectively, for the elevation and azimuth angles. We assume that $J = 3$ interferences are present: two of them are users of the system sharing the same resources as the UOI and one is a jamming station. They are located at 0.2° from the UOI and their INR are respectively 0, 0 and 10 dB. The output

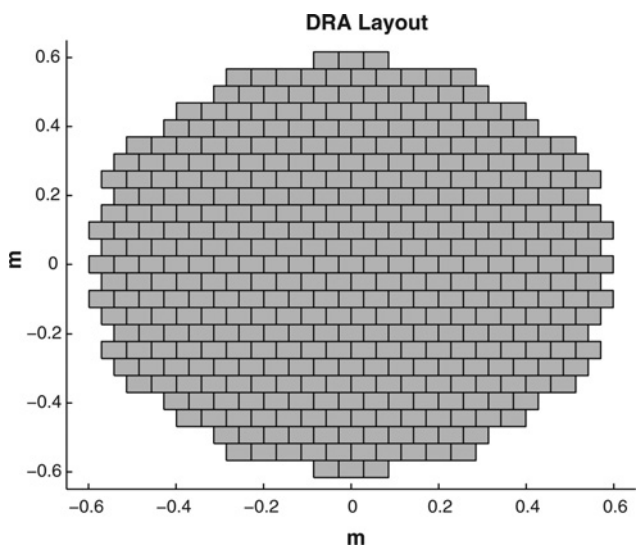

Figure 5 *Layout of the array*

SINR obtained with the conventional −non-adaptive− beamformer is −8.8 dB, which is considered as a value of reference we would like to enhance. Towards that end, it appears a need to consider adaptive beamformers. Besides, as concerns the UB beamformer, $L = 50$ random matrices $\mathbf{\Phi}$ are used to compute the weight vector.

4.2 MVDR scenario

In Figs. 6 and 7 we plot the average and worst-case output SINR against r. The number of snapshots is fixed to $N = 20$. The CG beamformer is possibly combined with diagonal loading, and the loading levels are either 10 or 20 dB above the white noise level.

Let us consider first the average SINR in Fig. 6. From inspection of this figure, it is clear that the CG beamformer achieves the best performance with the lowest number of iterations. As we already discussed, the maximum SINR is obtained for $r = J + 1 = 4$ iterations and comes very close to the optimum SINR which is equal to 37.5 dB. Moreover, once the iteration index exceeds $J + 1$, the SINR remains constant. This is a very appealing feature as one does not need to know exactly the number of interferences but only an upper-bound for this value in order to decide when the iterations should be stopped. Diagonal loading is not really helpful in this scenario and can even degrade the performance in case of a too large loading level. Regarding the AV beamformer, the following observations can be made. The SINR of the asymptotic AV beamformer $\boldsymbol{w}_{\mathrm{AV}-\infty}$ in (7) is very close to that obtained with the CG beamformer. This asymptotic regime is reached for $r = 60$ which is not very high but still larger than the number of iterations required by the CG beamformer. Therefore if the two beamformers have the same steady SINR, the CG converges faster. The UB beamformer has a lower maximum SINR than the two other

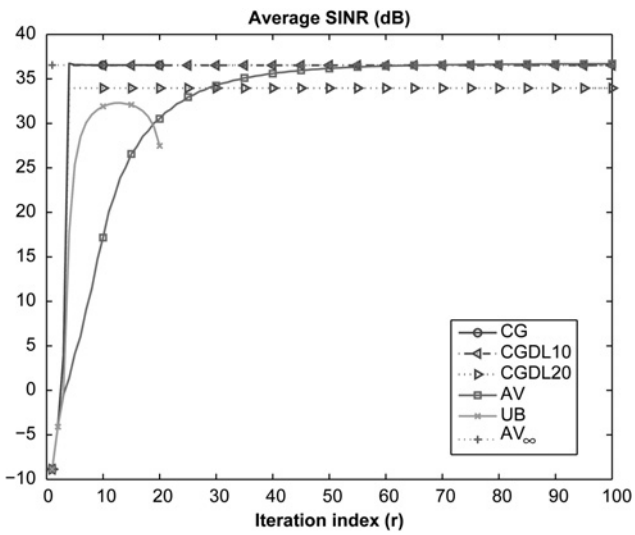

Figure 6 *MVDR scenario*
Average SINR against iteration index

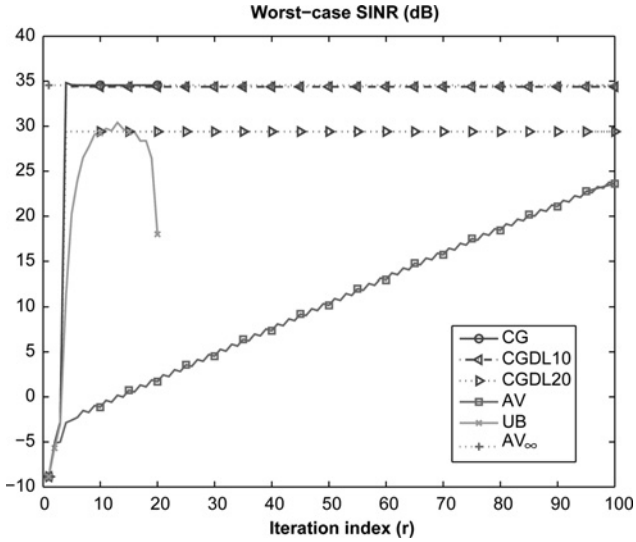

Figure 7 *MVDR scenario*
Worst-case SINR against iteration index

beamformers (note that r is kept lower than N, the rank of $\hat{\boldsymbol{R}}$, as $\mathbf{\Phi}^H \hat{\boldsymbol{R}} \mathbf{\Phi}$ must be invertible). Moreover, this maximum is achieved for $r \simeq 12$, which is larger than the actual size of the interference subspace. The reason for this is that the beamspace matrix $\mathbf{\Phi}$ is drawn randomly and hence a larger subspace dimension is required to include, with high probability, the true interference subspace. If r is too small $\mathbf{\Phi}$ may not capture the interference subspace, which results in poorer SINR. In order to improve the UB beamformer, the matrix $\mathbf{\Phi}$ should not be drawn completely at random but randomly within a spatial sector where the interferences are known to lie. This method, which would require some a priori information about the interferences localisation, may lead to some improvement. Since this is beyond the scope of the present paper, we do not elaborate further.

Regarding the worst-case SINR in Fig. 7, we can make the following comments. For all algorithms, except the AV beamformer, the worst-case SINR curves have the same characteristics as their average SINR counterparts, with a simple shift of about 2−3 dB, which indicates that the SINR are rather concentrated around their mean. In contrast, the worst-case SINR for the AV beamformer can be quite far from the average SINR, which shows a greater variability.

We now study the influence of the number of snapshots. Each algorithm is used with a 'close to optimal' value of r and the latter varies between the methods. As explained above, if J was known, one should use the CG with $r = J + 1$. Here we simply assume that an upper-bound of the number of interferences $J_{\mathrm{sup}} = 5$ is known and the CG algorithm is stopped at $r = J_{\mathrm{sup}} + 1$. The AV beamformer is stopped at $r = 40$, that is, before convergence in order to have a reasonable computational complexity. Finally, the UB beamformer is used with $r = 10$, so as to slightly overestimate the actual interference subspace dimension. Results are shown in Figs. 8 and 9, which confirms the

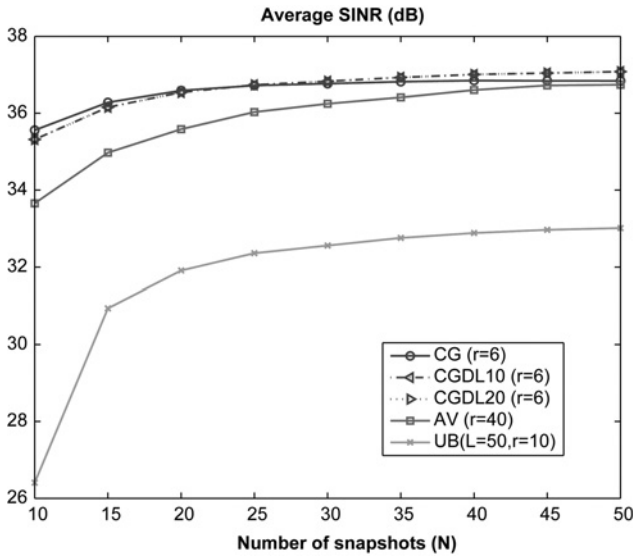

Figure 8 *MVDR scenario*

Average SINR against number of snapshots

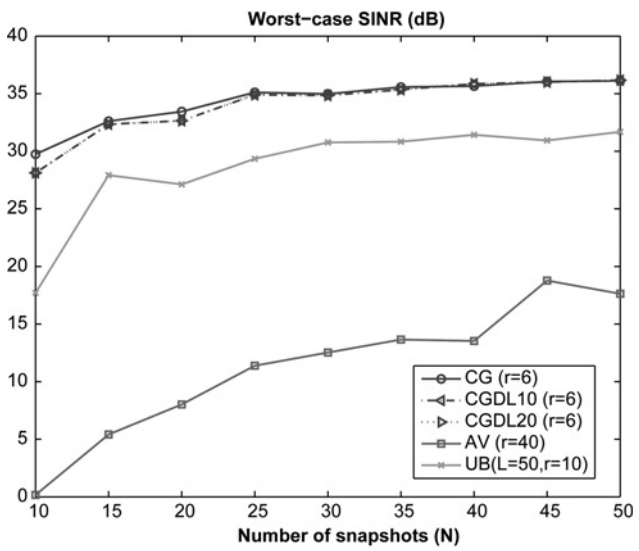

Figure 9 *MVDR scenario*

Worst-case SINR against number of snapshots

hierarchy established earlier, viz the CG beamformer is superior to the AV beamformer and the UB beamformer. Additionally, it can be observed that the MOE of the three beamformers is very good. More precisely, the CG and the AV beamformers attain the optimal SINR within 3 dB with only ten snapshots while slightly more snapshots are required for the UB beamformer. Finally, that the CG beamformer enjoys the smallest difference between average and worst-case SINR, followed by the UB beamformer and the AV beamformer.

4.3 MPDR scenario

We now consider that the SOI is present in the array measurements, in addition to the interferences and the noise. The SNR is set to 0 dB. Similarly to the previous case, we successively investigate the influence of r and N. In Figs. 10 and 11, we display the output SINR as a function of r, for $N = 20$.

Several observations can be made, that contrast with those made for the MVDR scenario.

- The CG still achieves its maximum SINR at $r = J + 1$ but, beyond this value, one can observe a significant drop of the SINR. Hence, in contrast to the MVDR scenario, the iterations should be stopped precisely at $r = J + 1$. Otherwise, a performance loss is incurred. In practice, this requires an accurate knowledge of the number of

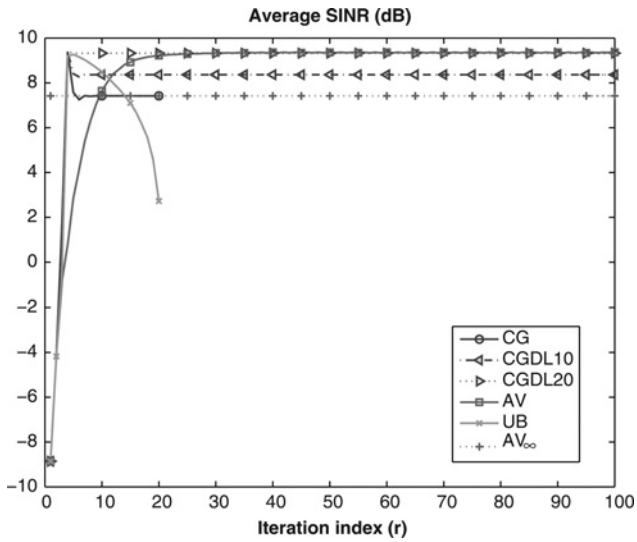

Figure 10 *MPDR scenario*

Average SINR against iteration index

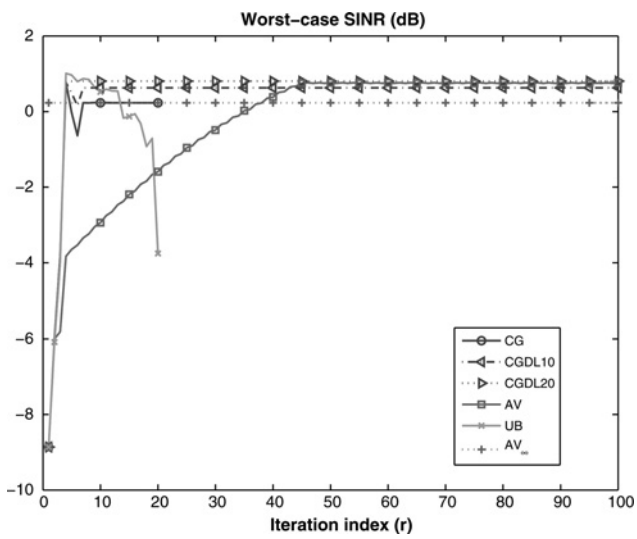

Figure 11 *MPDR scenario*

Worst-case SINR against iteration index

interferences, which is seldom available. Diagonal loading can be very helpful to alleviate this phenomenon, provided that the loading level is chosen properly. Indeed, for $\sigma^2_{\mathrm{DL}} = 10$ dB, one can still observe a SINR drop after $r = J + 1$ but this drop is limited and the steady-state SINR is better. With $\sigma^2_{\mathrm{DL}} = 20$ dB, the SINR remains constant. Therefore this simple modification we introduced in the CG beamformer tends to be effective. However, the choice of the loading level remains a delicate issue in practice.

- The AV beamformer has a performance equivalent to the best CG−DL beamformer and reaches a close to maximum possible SINR very quickly, viz $r = 30$ in this case. Therefore it is a very interesting method since no parameter such as σ^2_{DL} needs to be chosen. Moreover, it is not required to choose r with a high degree of accuracy −the SINR is constant in Fig. 10 from $r = 30$ to $r = 100$− which is very appealing. We would like to emphasise that at $r = 100$ the AV beamformer is still in a 'transient' behaviour as the SINR obtained with $\boldsymbol{w}_{\mathrm{AV}-\infty}$ is equivalent to that of the CG beamformer. It means that if r was increased further, the SINR of the AV beamformer would decrease and would converge to the SINR of $\boldsymbol{w}_{\mathrm{AV}-\infty}$ as $r \to \infty$. Consequently, there is a double advantage not to increase r too much, in terms of SINR and computational load.

- The UB beamformer exhibits a similar behaviour as in the MVDR scenario, except that the maximum SINR is achieved for $r = 6$. However, when r increases too much the SINR drops.

- The difference between the average SINR and the worst-case SINR is more pronounced than in the MVDR scenario. Indeed while the average SINR is around 8−9 dB, the worst-case SINR are around 0 dB. Again, the AV exhibits the largest difference.

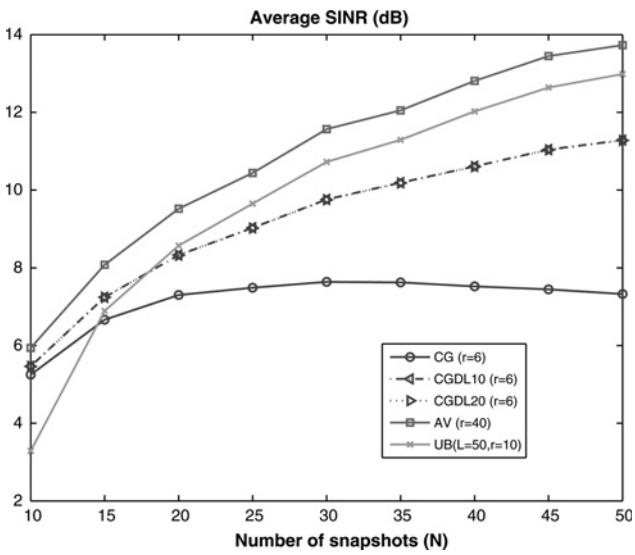

Figure 12 *MPDR scenario*
Average SINR against number of snapshots

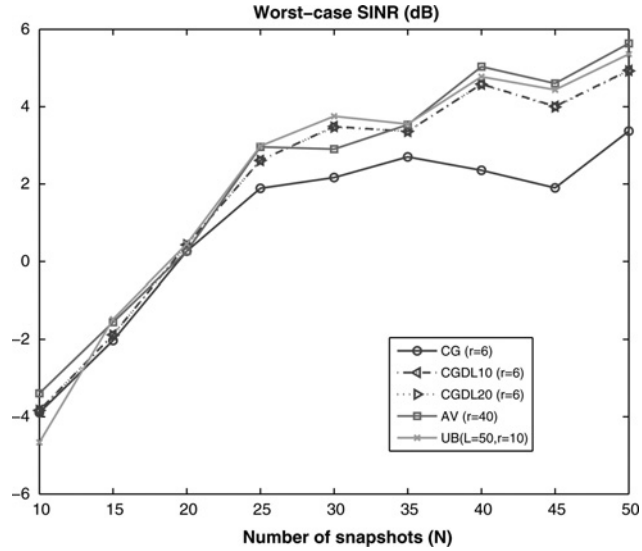

Figure 13 *MPDR scenario*
Worst-case SINR against number of snapshots

Figs. 12 and 13 display the output SINR against the number of snapshots. One can observe that the AV beamformer provides the highest SINR and outperforms the CG beamformer. The performance of the latter does not really improve when N is increased, mainly because r is not matched to $J + 1$. Introducing diagonal loading leads to some improvement of the SINR but, again, σ^2_{DL} should be chosen properly. The UB beamformer performs very well. Even if $r = 10$ is not an optimal choice for the UB beamformer, its SINR is better than that of the CG for $N \geq 20$ and is close to the best SINR.

4.4 Summary about the simulations results

To conclude this section, we can make the following remarks:

- In a MVDR scenario, the CG appears to be the method of choice. It converges very quickly in r and N, enables one to achieve a close to optimal SINR and does not need to know the exact number of interferences (only an upper-bound).

- In a MPDR scenario, the hierarchy is not as clear. The AV beamformer has a very good performance without requiring any user-parameter to tune. Its transient behaviour enables to obtain the highest SINR and it is rather robust to the choice of r. Diagonal loading is very helpful for the CG beamformer but the issue of selecting σ^2_{DL} is delicate. Without diagonal loading, the CG beamformer does not perform as well as the AV beamformer.

- The UB beamformer is potentially very interesting but the choice of the 'random' matrices $\boldsymbol{\Phi}$ needs to be investigated further in order to obtain some improvement. In fact, the matrices $\boldsymbol{\Phi}$ are drawn randomly and therefore they are likely to focus on spatial sectors which do not contain all

interferences. It then results that a larger number L of matrices should be averaged in order for all interferences to be captured. In order to improve the UB beamformer (and reduce L), it would be interesting, if available, to use some a priori information about the location of the interferers so as to draw matrices $\mathbf{\Phi}$ not isotropically but selectively in order for the beams drawn to contain the interferers with higher probability.

5 Conclusions

In this paper, we showed the feasibility of a satellite communications system that offers a global coverage for dispersed users and that allows one to optimise SINR and radio resource utilisation efficiency. This was achieved with the use of a large antenna array coupled with adaptive beamforming. We proposed three iterative, computationally efficient, and fast-converging beamformers that can provide good SINR with a very limited number of snapshots. In a MVDR scenario, we showed that the CG beamformer provides the best performance, at least when a tight upper-bound of the number of interferences is known. In a MPDR scenario, the AV beamformer is advocated as it is robust to the choice of the number of iterations.

6 Acknowledgment

This work was supported by the Délégation Générale pour l'Armement (DGA) and by Thales Alenia Space.

7 References

[1] JACOMB-HOOD A., LIER E.: 'Multibeam active phased arrays for communications satellites', *IEEE Microw. Mag.*, 2000, **1**, (4), pp. 40–47

[2] HAARDT C., ROUSSET D.: 'Flexible processor solutions for satellite communications'. Proc. ESA Workshop on Advanced Flexible Telecom Payload, ESA/ESTEC, Noordwijk, The Netherlands, 18–20 November 2008

[3] CRAIG T., BISHOP A., LEONG C., *ET AL.*: 'Flexible processor solutions for satellite communications'. Proc. ESA Workshop on Advanced Flexible Telecom Payload, ESA/ESTEC, Noordwijk, The Netherlands, 18–20 November 2008

[4] SOW G.: 'Méthodes d'Accès multiple a répartition spatiale pour communications par satellite'. PhD thesis, Ecole Nationale Supérieure des Télécommunications, 2006

[5] SOW G., BESSON O., BOUCHERET M.-L., GUIRAUD C.: 'Beamforming for satellite communications in emergency situations', *Eur. Trans. Telecommun.*, 2008, **19**, (2), pp. 161–171

[6] GUIRAUD C., ROUSSET D., ALBERT I.: 'Digital beamforming for multimedia flexible antennas'. Proc. 17th Int. Conf. Applied Electromagnetics and Communications, 2003, pp. 366–369

[7] GUY R.F.E., WYLLIE C.B., BRAIN J.R.: 'Synthesis of the inmarsat 4 multibeam mobile antenna'. Proc. 12th Int. Conf. Antennas and Propagation, 2003, vol. 1, pp. 90–93

[8] KOJIMA N., KITAO S., SHIRAMATSU K., YAJIMA M., SHIMADA M., NAKAMURA Y.: 'Development results of a proto flight model of the ka-band active phased array antenna for winds'. Proc. First European Conf. on Antennas and Propagation, 6–10 November 2006, pp. 1–5

[9] MAILLOUX R.J.: 'Phased array antennas handbook' (Artech House, Inc., 1994, 2nd edn.)

[10] GUIRAUD C., CAILLOCE Y., CAILLE G.: 'Reducing direct radiating array complexity by thinning and splitting itno non-regular subarrays'. Proc. 29th ESA Antenna Workshop on Multiple Beams and Reconfigurable Antennas, ESA/ESTEC, Noordwijk, The Netherlands, 18–20 April 2007

[11] VAN TREES H.L.: 'Optimum array processing' (John Wiley, New York, 2002)

[12] REED I.S., MALLETT J.D., BRENNAN L.E.: 'Rapid convergence rate in adaptive arrays', *IEEE Trans. Aerosp. Electron. Syst.*, 1974, **10**, (6), pp. 853–863

[13] BOROSON D.M.: 'Sample size considerations for adaptive arrays', *IEEE Trans. Aerosp. Electron. Syst.*, 1980, **16**, (4), p. 446–451

[14] FELDMAN D.D., GRIFFITHS L.J.: 'A projection approach for robust adaptive beamforming', *IEEE Trans. Signal Process.*, 1994, **42**, (4), pp. 867–876

[15] CARLSON B.D.: 'Covariance matrix estimation errors and diagonal loading in adaptive arrays', *IEEE Trans. Aerosp. Electron. Syst.*, 1988, **24**, (4), pp. 397–401

[16] LI J., STOICA P., WANG Z.: 'On robust Capon beamforming and diagonal loading', *IEEE Trans. Signal Process.*, 2003, **51**, (7), pp. 1702–1715

[17] VOROBYOV S.A., GERSHMAN A.B., LUO Z.-Q.: 'Robust adaptive beamforming using worst-case performance optimization: a solution to the signal mismatch problem', *IEEE Trans. Signal Process.*, 2003, **51**, (2), pp. 313–324

[18] LI J., DU L., STOICA P.: 'Fully automatic computation of diagonal loading levels for robust adaptive beamforming'. Proc. ICASSP, Las Vegas, NV, April 2008, pp. 2325–2328

[19] GUERCI J.R., GOLDSTEIN J.S., REED I.S.: 'Optimal and adaptive reduced-rank STAP', *IEEE Trans. Aerosp. Electron. Syst.*, 2000, **36**, (2), pp. 647–663

[20] PECKHAM C.D., HAIMOVICH A.M., AYOUB T.F., GOLDSTEIN J.S., REED I.S.: 'Reduced-rank STAP performance analysis', *IEEE Trans. Aerosp. Electron. Syst.*, 2000, **36**, (2), pp. 664–676

[21] HAIMOVICH A.M., BAR-NESS Y.: 'An eigenanalysis interference canceler', *IEEE Trans. Acoust. Speech Signal Process.*, 1991, **39**, (1), pp. 76–84

[22] HAIMOVICH A.M.: 'The eigencanceler: adaptive radar by eigenanalysis methods', *IEEE Trans. Aerosp. Electron. Syst.*, 1996, **32**, (2), pp. 532–542

[23] GOLDSTEIN J.S., REED I.S.: 'Subspace selection for partially adaptive sensor array processing', *IEEE Trans. Aerosp. Electron. Syst.*, 1997, **33**, (2), pp. 539–544

[24] GOLUB G., VAN LOAN C.: 'Matrix computations' (John Hopkins University Press, Baltimore, 1996, 3rd edn.)

[25] GOLDSTEIN J.S., REED I.S., SCHARF L.L.: 'A multistage representation of the wiener filter based on orthogonal projections', *IEEE Trans. Inf. Theory*, 1998, **44**, (7), pp. 2943–2959

[26] HONIG M.L., XAO W.: 'Performance of reduced-rank linear interference suppression', *IEEE Trans. Inf. Theory*, 2001, **47**, (5), pp. 1928–1946

[27] PADOS D.A., KARYSTINOS G.N.: 'An iterative algorithm for the computation of the MVDR filter', *IEEE Trans. Signal Process.*, 2001, **49**, (2), pp. 290–300

[28] QIAN H., BATALAMA S.N.: 'Data record-based criteria for the selection of an auxiliary vector estimator of the MMSE/MVDR filter', *IEEE Trans. Commun.*, 2003, **51**, (10), pp. 1700–1708

[29] PADOS D.A., KARYSTINOS G.N., BATALAMA S.N., MATYJAS J.D.: 'Short-data-record adaptive detection'. Proc. IEEE Radar Conf., Boston, MA, 17–20 April 2007, pp. 357–361

[30] BESSON O., MONTESINOS J., LARUE DE TOURNEMINE C.: 'On convergence of the auxiliary- vector beamformer with rank-deficient covariance matrices', *IEEE Signal Process. Lett.*, 2009, **16**, (4), pp. 249–252

[31] MARZETTA T.L., SIMON S.H., REN H.: 'Capon-MVDR spectral estimation from singular data covariance matrix, with no diagonal loading'. Proc. 14th Adaptive Sensor Array Processing Workshop, Lexington, MA, 6–7 June 2006